

logically since ozonations of phenolic solutions have been shown to produce hydroxyl radicals.⁴⁰ Methionine also has been shown to be susceptible to ozonation.^{41,42}

Our data indicate that the more reactive amino acid residues and PUFA are comparable in reactivity toward ozone. However, the proportion of attack on amino acids and PUFA in vivo cannot be deduced from rate data alone, since these rate studies do not take the effects of the microenvironment into account. The cellular geometry undoubtedly determines the accessibility of ozone to a potential substrate, and perhaps also the nature of the damage done by ozonation of the substrate. Additionally, the possibility of a single molecule of ozone causing damage to more than one substrate must be considered. It is known that ozone initiates the autoxidation of PUFA and this can cause the cooxidation of other materials, such as proteins, that are present. Furthermore, PUFA autoxidation produces harmful byproducts such as malonaldehyde that can crosslink proteins.⁴³ It is also possible that harmful byproducts such as singlet oxygen or oxidized derivatives of amines (such as nitro or nitroso compounds, hydroxylamines, or imino

acids) could be produced from the ozonation of proteins or peptides,¹⁸ which could cause further damage. Thus, although this compilation of rate constants does not allow one to rank the biological risk of all the potential target molecules, it does serve as a guide for further studies.

Acknowledgment. This work was supported in part by grants from the NIH (HL-16029) and the National Science Foundation. We would like to thank Dr. E. W. Blakeney for performing the amino acid analyses.

Registry No. Leucine, 61-90-5; isoleucine, 73-32-5; alanine, 56-41-7; valine, 72-18-4; glycine, 56-40-6; phenylalanine, 63-91-2; proline, 147-85-3; glutamic acid, 56-86-0; glutamine, 56-85-9; aspartic acid, 56-84-8; asparagine, 70-47-3; arginine, 74-79-3; threonine, 72-19-5; serine, 56-45-1; lysine, 56-87-1; histidine, 71-00-1; cysteine, 52-90-4; methionine, 63-68-3; tryptophan, 73-22-3; butylamine, 109-73-9; *tert*-butylamine, 75-64-9; *sec*-butylamine, 13852-84-6; benzylamine, 100-46-9; diethylamine, 109-89-7; triethylamine, 121-44-8; imidazole, 288-32-4; 4-methylimidazole, 822-36-6; *N*- α -acetyllysine, 1946-82-3; *N*- ϵ -acetyllysine, 692-04-6; *N*- α -acetylhistidine, 2497-02-1; glutathione, 70-18-8; methionine sulfoxide, 454-41-1; methionine sulfone, 1118-85-0; maleic acid, 110-16-7; 2-hexenoic acid, 1191-04-4; pivalic acid, 75-98-9; ethanol, 64-17-5; 2-propanol, 67-63-0; 1-butanol, 71-36-3; sucrose, 57-50-1; tetrahydrofuran, 109-99-9; acrylonitrile, 107-13-1; *N,N*-dimethylacetamide, 127-19-5; *N*-methylacetamide, 79-16-3; dimethyl sulfoxide, 67-68-5; *N*-acetylglycine, 543-24-8; *N*-acetylserine, 16354-58-8; tyrosine, 60-18-4; 3-hexenoic acid, 4219-24-3.

(40) Grimes, H. D.; Perkins, K. K.; Boss, W. F. *Plant Physiol.* **1983**, *72*, 1016-1020.

(41) Dooley, M. M.; Mudd, J. B. *Arch. Biochem. Biophys.* **1982**, *218*, 459-471.

(42) Leh, F.; Warr, T. A.; Mudd, J. B. *Environ. Res.* **1978**, *16*, 179-190.

(43) Chio, K. S.; Tappel, A. L. *Biochemistry* **1969**, *8*, 2827-2832, and references therein.

Kinetics and Mechanism of Aromatic Thallation. Identification and Proof of Competing Electrophilic and Electron-Transfer Pathways

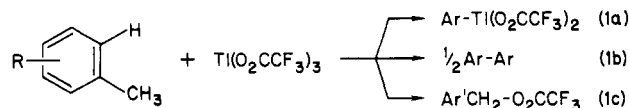
W. Lau and J. K. Kochi*

Contribution from the Departments of Chemistry, University of Houston, Houston, Texas 77004, and Indiana University, Bloomington, Indiana 47405. Received May 10, 1984

Abstract: The unusual occurrence of simultaneous electrophilic (two-electron) and electron-transfer (one-electron) pathways during the thallation of the homologous methylbenzenes ArCH_3 is demonstrated by (1) the careful analysis and identification of three major types of products, (2) the complete dissection of the complex kinetics, and (3) the identification of the reactive intermediates by time-resolved UV-vis and ESR spectroscopy. Side-chain substitution S, dimerization D, and oxidative nuclear substitution O derive from the radical cation $\text{ArCH}_3^{\cdot+}$ produced as a common intermediate by electron transfer from the methylbenzene to thallium(III) trifluoroacetate in trifluoroacetic acid. The importance of $\text{ArCH}_3^{\cdot+}$, which is detected by both its electronic and ESR spectra, decreases in the following order, hexamethylbenzene > pentamethylbenzene > durene >> mesitylene, with a concomitant rise in electrophilic nuclear thallation R to account for the complete material balance. The striking color changes that accompany thallation are identified as charge-transfer transitions in the series of transient 1:1 π -complexes of the methylbenzene donors and the thallium(III) acceptor. Quantitative spectrophotometry employing the Benesi-Hildebrand analysis establishes the cationic $\text{Tl}(\text{O}_2\text{CCF}_3)_2^+$ formed by the dissociation of a single trifluoroacetate ligand from the parent thallium tris(trifluoroacetate) as the active electron acceptor. The complete analysis of the complex kinetics including kinetic isotope effects which accompany the nuclear thallation R of mesitylene as well as the side-chain substitution S of hexamethylbenzene shows that the cationic $\text{Tl}(\text{O}_2\text{CCF}_3)_2^+$ also serves the dual function as the active electrophile and the active oxidant, respectively. The close competition between these apparently disparate pathways is quantitatively evaluated by the second-order rate constants which differ by less than an order of magnitude. Therefore, the thallation of aromatic hydrocarbons represents one of the few systems in which such dual pathways, electrophilic and free radical, apparently occur side by side under the same experimental conditions of solvent, temperature, etc. Accordingly, it represents an unusual opportunity to delineate two-electron (concerted, electrophilic) from one-electron (stepwise, free radical) mechanisms—especially as to whether they represent parallel or sequential events.

The pioneering studies of Taylor, McKillop, and co-workers^{1,2} have established the utility of thallium tris(trifluoroacetate) (TTFA) as a reagent in organic chemistry, particularly to effect a wide variety of aromatic transformations. In this regard, at least three major reactions have been identified in aromatic thallation:

namely, (a) nuclear substitution, (b) biaryl coupling, and (c) side-chain substitution, e.g.



* Address correspondence to this author at the University of Houston.

where $\text{Ar} = \text{R}(\text{CH}_3)_6\text{H}_3$ and $\text{Ar}' = \text{RC}_6\text{H}_4$. Although the nuclear thallation in eq 1a is commonly postulated to proceed via a traditional electrophilic mechanism,³ the reactions in eq 1b and 1c are considered to involve free radical intermediates.⁴ Indeed in an earlier ESR study of aromatic thallation, we demonstrated the presence of a variety of paramagnetic intermediates, which are formed simply upon mixing thallium(III) trifluoroacetate and an aromatic hydrocarbon.⁵

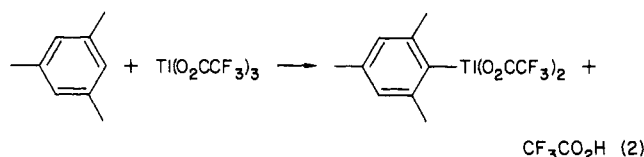
Heretofore, most of the studies relating to TTFA reactions with aromatic compounds have been directed toward synthetic objectives.^{1,2,6} Although there are a few sporadic reports of quantitative rate measurements,^{3,7,8} there is extant no comprehensive kinetic study encompassing the gamut of reactivities from the electron-rich arenes (such as hexamethylbenzene) to the electron-deficient ones. Moreover, the active thallating species responsible for reaction with aromatic hydrocarbons have not been identified. Accordingly, we wish to present in this study the products and stoichiometry, the spectroscopic examinations of the different intermediates, and a kinetic determination of the activation barriers for the diverse reactions of TTFA. We focus our attention on the homologous alkylbenzenes, since this series of related aromatic hydrocarbons are sufficient to differentiate the three major types of aromatic transformations described in eq 1.

Results

We proceed by first separating and then identifying the diverse products derived from the exposure of mesitylene, durene, pentamethylbenzene, and hexamethylbenzene to thallium tris(trifluoroacetate) (TTFA) in trifluoroacetic acid. We next examine the formation of labile π -complexes as reactive intermediates by probing the nature of the transient color changes accompanying the reactions of TTFA with various arenes by a quantitative examination of the spectral changes in the UV-vis absorption bands. This is followed by the rigorous solution of the complex kinetics which identifies the active thallating species and delineates the kinetic isotope effect in the rate-limiting process in relation to the color changes. Finally the detection of transient intermediates in this system is provided by the electron spin resonance (ESR) spectroscopic examination during the active course of aromatic thallation.

(I) Products and Stoichiometries of Aromatic Thallations.

When a colorless solution of thallium(III) trifluoroacetate in trifluoroacetic acid is mixed with mesitylene at ambient temperatures, the homogeneous mixture immediately takes on a yellow coloration—which bleaches completely as the thallation is finished within a few minutes. Rapid isolation of the products affords the thallated mesitylene⁹ in essentially quantitative yields according to the stoichiometry:



(1) (a) McKillop, A.; Fowler, J. S.; Zelesko, M. J.; Hunt, J. D.; Taylor, E. C.; McGillivray, G. *Tetrahedron Lett.* **1969**, 29, 2423. (b) McKillop, A.; Hunt, J. D.; Zelesko, M. J.; Fowler, J. S.; Taylor, E. C.; McGillivray, G.; Kienzie, F. J. *Am. Chem. Soc.* **1971**, 93, 4841. (c) Taylor, E. C.; Kienzie, F.; Robey, R. L.; McKillop, A.; Hunt, J. D. *Ibid.* **1971**, 93, 4845. (d) Taylor, E. C.; McKillop, A. *Acc. Chem. Res.* **1970**, 3, 338.

(2) McKillop, A.; Turrell, A. G.; Young, D. W.; Taylor, E. C. *J. Am. Chem. Soc.* **1980**, 102, 6504.

(3) Olah, G. A.; Hashimoto, I.; Lin, H. C. *Proc. Natl. Acad. Sci. U.S.A.* **1977**, 74, 4121.

(4) See ref 2 and Lau et al.: Lau, W.; Huffman, J. C.; Kochi, J. K. *J. Am. Chem. Soc.* **1982**, 104, 5515.

(5) Elson, I. H.; Kochi, J. K. *J. Am. Chem. Soc.* **1973**, 95, 5060.

(6) McKillop, A.; Taylor, E. C. *Adv. Organomet. Chem.* **1973**, 11, 147.

(7) (a) Henry, P. M. J. *Org. Chem.* **1970**, 35, 3083. (b) Briody, J. M.; Moore, R. A. *Chem. Ind. (London)* **1970**, 803. (c) Briody, J. M.; Moore, R. A. *J. Chem. Soc., Perkin Trans 2* **1972**, 179. (d) Kwok, P. Y.; Stock, L. M.; Wright, T. L. *J. Org. Chem.* **1979**, 44, 2309.

(8) (a) Roberts, R. M. G. *Tetrahedron* **1980**, 36, 3281. (b) Al-Azzawi, S. F.; Roberts, R. M. G. *J. Chem. Soc., Perkin Trans 2* **1982**, 677.

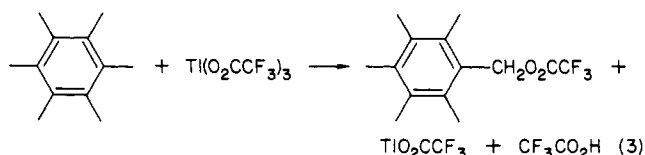
(9) Maher, M. P.; Evans, D. F. *J. Chem. Soc.* **1965**, 637.

Table I. Products Derived from Various Polymethylbenzenes and Thallium Tris(trifluoroacetate)^a

$\text{C}_6\text{H}_n(\text{CH}_3)_{6-n}$	recovered reactant ^b	products, ^c μmol		
		R	S	D
mesitylene	4.5	93	<1	<1
durene	27	47	2	7
pentamethylbenzene	23	26	7 ^d	12
hexamethylbenzene	<1		95	

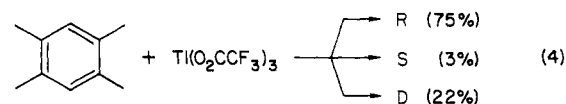
^a From a reaction consisting of TTFA (100 μmol), arene (100 μmol), and LiO_2CCF_3 (100 μmol) in 3 mL of trifluoroacetic acid at 25 °C. ^b Arene recovered after 2–3 h. ^c R = nuclear thallation product, D = dimeric aromatic hydrocarbon, S = benzylic trifluoroacetate. See Experimental Section for identification and analysis. ^d Includes both nuclear and benzylic trifluoroacetate isomers (see text).

A similar series of color changes also accompany the thermal reaction of the fully methylated analogue hexamethylbenzene with TTFA under the same conditions. However, with this arene, the product is exclusively pentamethylbenzyl trifluoroacetate together with the reduced thallium(I) trifluoroacetate, i.e.

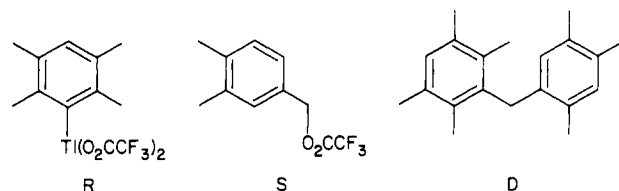


The formation of the benzylic ester as the sole product may not be unexpected owing to the absence of free ring positions in hexamethylbenzene. What is surprising, however, is that the side-chain substitution in eq 3 occurs at qualitatively the same rate as the nuclear substitution in eq 2. Nonetheless, the two types of products are clearly delineated—the nuclear thallation in eq 2 being the exclusive pathway uncontaminated by side-chain substitution leading to the benzylic ester 3,5-dimethylbenzyl trifluoroacetate.

Visually, the treatment of pentamethylbenzene and durene with TTFA proceeds in much the same way as that with mesitylene and hexamethylbenzene. The thallation reaction from durene upon workup, however, affords a mixture of three types of aromatic products, i.e.



Each of the components in the product mixture derived from durene was separated by gas chromatography and identified as:



[The details of the analysis are described in the Experimental Section.] Nuclear substitution R is thus analogous to eq 2 observed with mesitylene; and the side-chain substitution S is the counterpart to eq 3 with hexamethylbenzene. Moreover, the oxidative dimer D is akin to the biaryls derived previously from phenyl ethers.¹¹ [For convenience of identification, the nuclear thallation will be hereafter referred to generically as R, the side-chain substitution as S, and the dimer formation as D.]

Pentamethylbenzene with thallium(III) trifluoroacetate affords a similar mixture containing four types of products, three of which are analogous to those described in eq 4, albeit in different proportions as listed in Table I. The unique product is penta-

(10) Svanholm, U.; Parker, V. D. *Tetrahedron Lett.* **1972**, 471.

(11) See ref 2 and Taylor et al.: Taylor, E. C.; Andrade, J. G.; Rall, G. J. H.; McKillop, A. *J. Am. Chem. Soc.* **1980**, 102, 6513.

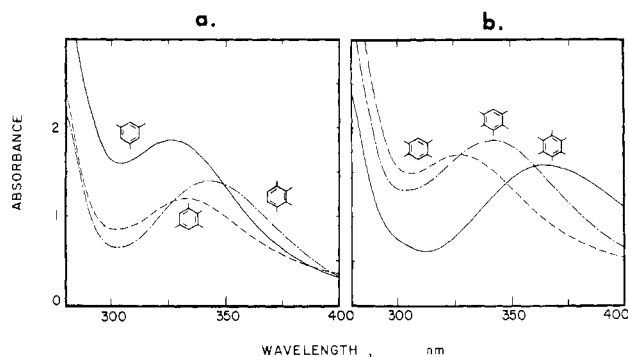
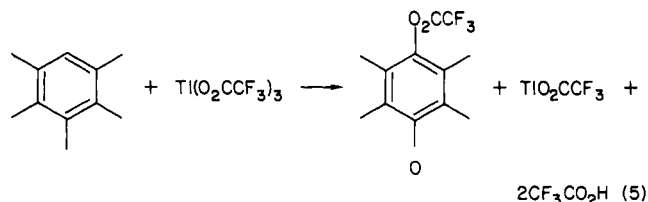


Figure 1. Transient charge-transfer absorption bands from various methylbenzenes and thallium(III) trifluoroacetate in trifluoroacetic acid at 25 °C. (a) TTFA (0.0060 M) and 0.0060 M prehnitene (---), TTFA (0.0045 M) and 0.0045 M isodurene (---), TTFA (0.015 M) and 0.015 M mesitylene (—). (b) TTFA (0.0015 M) and 0.0015 M hexamethylbenzene (—), TTFA (0.0050 M) and 0.0050 M pentamethylbenzene (---), and TTFA (0.012 M) and 0.012 M durene (---). Each contains 0.05 M lithium trifluoroacetate.

methylphenyl trifluoroacetate which corresponds to a process involving oxidative nuclear esterification (O), i.e.¹²



The yield of this aryl ester is highly dependent on the stoichiometric excess of TTFA. Thus the thallation of pentamethylbenzene in the presence of 2 equiv of TTFA affords more than a 50% yield of O, and there is a concomitant diminution in nuclear thallation to R and oxidative dimerization to D.¹⁴ However, the enhancement of O is nullified if 1 equiv of lithium trifluoroacetate is included. The effect of lithium trifluoroacetate on the product complexation is dependent on the structure of the arene, being most apparent with those which generate several types of products. Thus the thallation of mesitylene to produce R is not materially affected by added LiO₂CCF₃. Likewise, the yield of pentamethylbenzyl trifluoroacetate (S) from hexamethylbenzene is the same irrespective of the molar excess of TTFA and the presence or absence of added lithium trifluoroacetate.

(II) The Detection of Labile Arene-Thallium(III) Complexes via Transient Charge-Transfer Absorption Bands. The series of homologous methylbenzenes in Table I all share in common the appearance of transient colors when they are mixed with thallium(III) trifluoroacetate. The fleeting colors relate to absorption bands occurring in the UV-vis region of the electronic spectrum, as shown in Figure 1.¹⁵ In every case, the absorption maxima are clearly resolved from the long wavelength tails of either the parent methylbenzene or thallium(III) trifluoroacetate. [The latter are indicated by the strong absorptions below 300 nm.] The new absorption bands are uniformly broad and featureless, characteristic of charge-transfer or CT bands associated with intermolecular electron donor-acceptor or EDA complexes.¹⁶ Most importantly, the absorption bands ($h\nu_{CT}$) shift to progressively lower energies with the decrease in the ionization potential I_D of

Table II. Charge-Transfer Absorption Bands of π -Complexes of Aromatic Hydrocarbons with TTFA^a

arene	I_D , ^b eV	λ_{CT} , ^c nm
hexamethylbenzene	7.85	364
hexaethylbenzene	7.71	366
pentamethylbenzene	7.92	343
1,2,3,4-tetramethylbenzene	8.14	342
1,2,3,5-tetramethylbenzene	8.07	332
1,2,4,5-tetramethylbenzene	8.05	327
1,2,3-trimethylbenzene	8.42	337
1,2,4-trimethylbenzene	8.27	326
1,3,5-trimethylbenzene	8.42	327
1,2-xylene	8.56	330
1,3-xylene	8.56	326
1,4-xylene	8.44	311
<i>tert</i> -butylbenzene	8.65	330
isopropylbenzene	8.71	330
ethylbenzene	8.77	327
toluene	8.82	324
benzene	9.23	313

^a In trifluoroacetic acid solution at 25 °C. ^b Vertical ionization potential. ^c Charge-transfer band (λ_{max}).

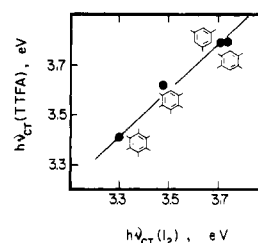


Figure 2. The charge-transfer interaction of thallium(III) trifluoroacetate and various polymethylbenzenes in trifluoroacetic acid solutions. The direct comparison of the absorption bands ($h\nu_{CT}$) derived from thallium(III) trifluoroacetate with those from iodine and the same polymethylarene donors as indicated.

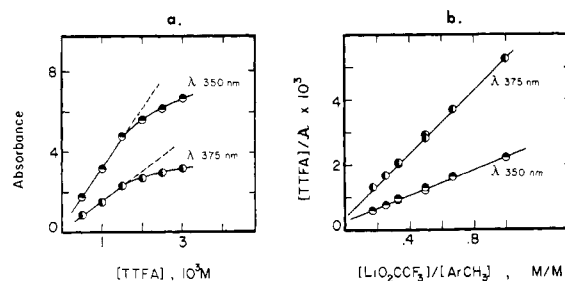


Figure 3. Benesi-Hildebrand plots of charge-transfer absorbances from various concentrations of polymethylbenzenes and thallium(III) trifluoroacetate in trifluoroacetic acid according to (a) eq 7 and (b) eq 10.

the aromatic donors listed in Table II. Indeed the direct relationship between $h\nu_{CT}$ and I_D for the methylbenzenes is strongly diagnostic of the charge-transfer origin of these transient absorption bands.¹⁷ This conclusion is supported by the comparison in Figure 2 of these absorption bands with those associated with the classic arene-iodine EDA complexes discovered by Benesi and Hildebrand¹⁸ and whose structure has been established by X-ray crystallography.¹⁹

In order to quantitatively assess the importance of the arene-thallium(III) π -complexes formed under these conditions, we employed the method originally developed by Benesi and Hildebrand²⁰ for the spectrophotometric determination of the formation constant K and the extinction coefficient ϵ_{DA} relating to the

(12) Compare eq 5 with a comparable transformation with cobaltic trifluoroacetate.¹³

(13) Kochi, J. K.; Tang, R. T.; Bernath, T. *J. Am. Chem. Soc.* **1973**, *95*, 7114.

(14) Further details of the effect of added trifluoroacetate on TTFA reactions will be reported later.

(15) With some arenes, the final reaction mixtures are tinged with a pink-red coloration (vide infra).

(16) Mulliken, R. S.; Person, W. B. "Molecular Complexes"; Wiley: New York, 1969.

(17) Foster, R. "Organic Charge Transfer Complexes"; Academic Press: New York, 1969.

(18) (a) Benesi, H. A.; Hildebrand, J. H. *J. Am. Chem. Soc.* **1949**, *71*, 2703. (b) Person, W. B. *Ibid.* **1965**, *87*, 167.

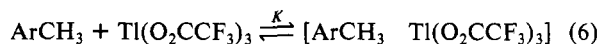
(19) Cf.: Hassel, O.; Stromme, K. O. *Acta Chem. Scand.* **1959**, *13*, 1781; **1958**, *12*, 1146. See also: Prout, C. K. "Molecular Complexes"; Foster, R., Ed.; Crane, Russak & Co.: New York, 1973; Vol. I, pp 151 ff.

Table III. Variations in the Charge-Transfer Absorbance with Changes in the Concentration (M) of the Polymethylbenzene Donor and Thallium(III) Trifluoroacetate Acceptor^a

TTFA	mesitylene	LiO ₂ CCF ₃	absorbance ^b	
			375	350
0.00050	0.020	0	0.81	1.68
0.0010	0.020	0	1.52	3.18
0.0015	0.020	0	2.30	4.78
0.0020	0.020	0	2.68	5.56
0.0025	0.020	0	2.94	6.12
0.0030	0.020	0	3.20	6.64
0.0020	0.060	0.010	1.54	3.57
0.0020	0.040	0.010	1.20	2.67
0.0020	0.030	0.010	0.97	2.20
0.0020	0.020	0.010	0.71	1.65
0.0020	0.060	0.020	0.95	2.17
0.0020	0.040	0.020	0.68	1.59
0.0020	0.030	0.020	0.54	1.27
0.0020	0.020	0.020	0.38	0.90

^a In trifluoroacetic acid at 25 °C. ^b At the monitoring wavelength (nm) absorbances at 350 nm were measured with a 2-mm cuvette and converted to a 10-mm scale.

charge-transfer band. Let us first consider a straightforward equilibrium between the methylbenzenes [ArCH₃] with thallium(III) trifluoroacetate, i.e.,

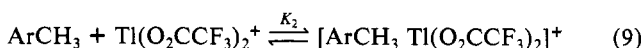


In the formation of such simple 1:1 complexes, the changes in the absorbances \mathcal{A}_{CT} of the charge-transfer bands resulting from variations in the donor and acceptor concentrations is given by the expression

$$\frac{[\text{TTFA}]}{\mathcal{A}_{\text{CT}}} = \frac{1}{\epsilon_{\text{DA}}} + \frac{1}{K\epsilon_{\text{DA}}} \frac{1}{[\text{ArCH}_3]} \quad (7)$$

under conditions in which $[\text{ArCH}_3] \gg [\text{TTFA}]$.²¹ The results are presented in Table III for mesitylene as a typical methylbenzene donor. At a given concentration of $[\text{ArCH}_3]$, the Benesi-Hildebrand plot in Figure 3a is not linear as predicted by eq 7. This clearly indicates that the molar absorptivity of the charge-transfer band actually increases with decreasing initial concentrations of thallium(III) trifluoroacetate. Such behavior suggests a dissociative phenomenon leading to the charge-transfer absorption bands. Accordingly, the straightforward complex formation in eq 6 was reconsidered as a pair of equilibria:

Scheme I

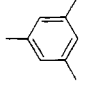
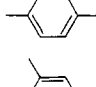
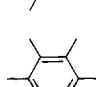
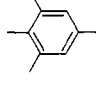
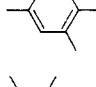
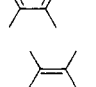
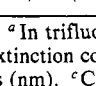
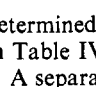


in which the concentration of trifluoroacetate anion is introduced as a new variable. It can be readily modulated by the deliberate addition of lithium trifluoroacetate. If Scheme I is applicable, the Benesi-Hildebrand relationship for the CT absorption changes accompanying the formation of the cationic complex $[\text{ArCH}_3 \text{ Ti}(\text{O}_2\text{CCF}_3)_2]^+$ is given by the expression:

$$\frac{[\text{TTFA}]}{\mathcal{A}_{\text{CT}}} = \frac{1}{\epsilon_{\text{DA}}} + \frac{K_1 + [\text{LiO}_2\text{CCF}_3]}{K_1 K_2 \epsilon_{\text{DA}} [\text{ArCH}_3]} \quad (10)$$

The fit of the data to this formulation is illustrated in Figure 3b by a line with a slope determined by the constants $(K_1 K_2 \epsilon_{\text{DA}})^{-1}$ and an intercept of $\epsilon_{\text{DA}}^{-1}$ under conditions in which $K_1 \ll [\text{LiO}_2\text{CCF}_3]$, as described in Table III. Two monitoring wavelengths of 350 and 375 nm were chosen for an optimum measurement of the absorbance changes between 0.5 and 2.0 at various concentrations of mesitylene and thallium(III) trifluoroacetate. The equilibrium constant product $K_1 K_2$ thus obtained was indeed found to be independent of the monitoring wavelength—being 0.127 and 0.133 at 375 and 350 nm, respectively. The values of $K_1 K_2$

Table IV. Formation Constants for the EDA Complexes of Methylbenzene and Thallium(III) Trifluoroacetate by the Benesi-Hildebrand Method^a

methylbenzene	$\epsilon(\lambda),^b$ M ⁻¹ cm ⁻¹ (nm)	$K_1 K_2$	$K_2,^c$ M ⁻¹
	1970 (375), 4090 (350)	0.13	130
	2322 (360)	0.057	57
	3035 (385)	0.076	76
	2147 (395)	0.50	500
	1091 (395)	0.38	380
	2263 (390)	0.067	67
	3526 (395)	1.64	1640
	4694 (330)	2.45	2450

^a In trifluoroacetic acid containing lithium trifluoroacetate. ^b Molar extinction coefficient at the monitoring wavelength given in parentheses (nm). ^c Calculated from the values in the third column, assuming $K_1 = 1 \times 10^{-3}$ M.

determined in this manner for various methylbenzenes are listed in Table IV.

A separate evaluation of the dissociation constant $K_1 \approx 5 \times 10^{-4}$ M for the ionization of thallium(III) trifluoroacetate was obtained from an explicit solution of eq 10 at various concentrations of lithium trifluoroacetate. However, there is likely to be a substantial uncertainty in this magnitude of K_1 since it is too small compared to the lithium trifluoroacetate concentration of 0.01–0.04 M for the formulation given in eq 10 to yield accurate results. Nonetheless, an upper limit for K_1 can be estimated to be $< 1 \times 10^{-3}$ M.²² This value together with those evaluated for $K_1 K_2$ afforded the formation constants K_2 for the EDA complexes of various methylbenzenes with $\text{Ti}(\text{O}_2\text{CCF}_3)_2^+$, which are listed in the last column in Table IV.

In order to establish whether the undissociated $\text{Ti}(\text{O}_2\text{CCF}_3)_3$ also participates directly in the formation of arene π -complexes, the molar absorptivity of the CT band arising from mesitylene and TTFA was investigated at three wavelengths of 328, 360, and 375 nm at various trifluoroacetate concentrations. The three wavelengths monitored encompass the envelope of the CT band. The results illustrated in Figure 4 provide unambiguous evidence that only one absorption band is involved. We thus conclude that the undissociated $\text{Ti}(\text{O}_2\text{CCF}_3)_3$ plays no active role as an acceptor in forming a π -complex other than merely serving as the precursor for the active agent in eq 8.

(20) See ref 17, 18 and Foster: Foster, R. "Molecular Complexes"; Foster, R., Ed.; Crane Russak & Co.: New York, 1974; Vol. 2, pp 107 ff.

(21) Under these conditions, the change in arene concentration is negligible.

(22) Since $K_1 \ll [\text{LiO}_2\text{CCF}_3]$ in eq 10, the uncertainty in the measured value of $K_1 = 5 \times 10^{-4}$ may be as large as a factor of 2.

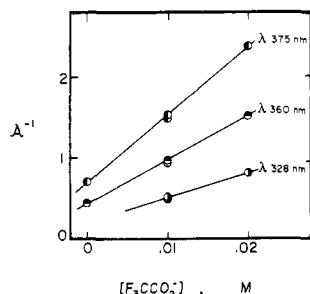


Figure 4. Homogeneity of the charge-transfer absorption band arising from mesitylene and TTFA by the wavelength dependence of the absorbance with trifluoroacetate concentration.

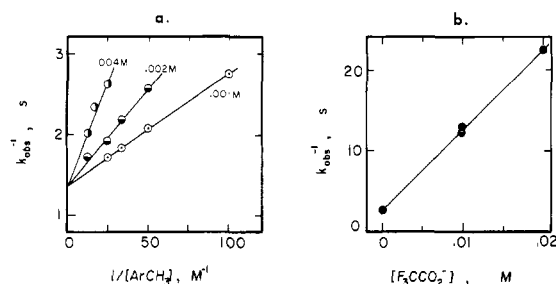


Figure 5. The effect of thallium(III) trifluoroacetate concentrations on the pseudo-first-order rate constant for mesitylene thallation in trifluoroacetic acid. (a) Michaelis-Menten behavior with the variation in mesitylene concentration according to eq 11. [TTFA] = 0.004 M (●), 0.002 M (○), 0.001 M (○). (b) Variation in the pseudo-first-order rate constant with the concentration of added lithium trifluoroacetate. [Mesitylene] = 0.02 M, [TTFA] = 0.002 M.

(III) Kinetics of Aromatic Thallation—The Nature of the Active Thallating Agent. The unambiguous stoichiometry for the thallation of mesitylene (see eq 2) permitted us to examine the kinetics of this prototypical system in detail. The rates of reaction could be measured by following the changes in the concentration of mesitylene and/or the product mesitylthallium bis(trifluoroacetate) with use of the characteristic ^1H NMR resonances at δ 2.33 [$J(\text{Ti}, \text{CH}_3) = 61$ Hz] and δ 2.72 [$J(\text{Ti}, \text{CH}_3) = 120$ Hz], for the *p*- and *o*-methyl groups, respectively.²³ Alternatively, we could follow the temporal changes in the absorbance of the charge-transfer band at 355 nm for the mesitylene-thallium(III) trifluoroacetate EDA complex (vide supra). In either case, the thallation of mesitylene was found to follow overall second-order kinetics, being first order in each component in accord with previous kinetic studies with benzene and toluene.^{7,8} Accordingly, all further kinetic studies were carried out by the CT method since the availability of the rapid-scan spectrometer with a 0.1-s time resolution allowed us to examine an enlarged span of rates.

At a particular concentration of TTFA and under conditions in which $[\text{ArCH}_3] \gg [\text{TTFA}]$, the pseudo-first-order constant k_{obsd} obeys a relationship of the form:

$$\frac{1}{k_{\text{obsd}}} = \frac{1}{k} + \frac{1}{Kk[\text{ArCH}_3]} \quad (11)$$

as presented in Table V. Such a Michaelis-Menten behavior of the rate constant is in accord with the formation of the EDA complexes described in the foregoing section.²⁴ The results in Figure 5a show, however, that the pseudo-first-order rate constant actually decreases with increasing concentrations of TTFA. The common intercept suggests that the unusual kinetic behavior is related to a pre-equilibrium dissociation, reminiscent of that described in eq 8. Indeed further experiments carried out in the

Table V. Effect of Thallium(III) and Trifluoroacetate Concentrations (10^2 M) on the Rate of Mesitylene Thallation^a

TTFA	mesitylene	LiO_2CCF_3	$k_{\text{obsd}}, \text{s}^{-1}$	k, s^{-1}	K, M^{-1}
1.00	1.00	0	0.36		
1.00	2.00	0	0.48	0.73	100
1.00	3.00	0	0.55		
1.00	4.00	0	0.58		
2.00	2.00	0	0.38		
2.00	3.00	0	0.46	0.76	50.2
2.00	4.00	0	0.52		
2.00	8.00	0	0.58		
4.00	4.00	0	0.38		
4.00	6.00	0	0.43	0.68	31.7
4.00	8.00	0	0.50		
1.00	1.00	2.00	0.026		
1.00	3.00	2.00	0.066		
2.00	2.00	1.00	0.080		
2.00	2.00	2.00	0.047		
2.00	2.00	2.00 ^c	0.049		
2.00	3.00	2.00	0.065		
4.00	4.00	2.00	0.077		
4.00	8.00	2.00	0.14		

^a In 2.00 mL of trifluoroacetic acid at 25 °C. ^b Calculated according to eq 11. ^c In the presence of added LiClO_4 (2.00×10^{-2} M).

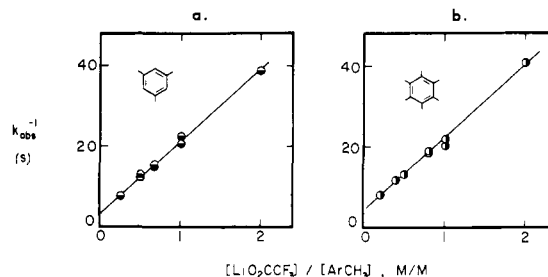


Figure 6. The generalized kinetics according to eq 12 of (a) the nuclear thallation of mesitylene and (b) the side-chain substitution of hexamethylbenzene at various concentrations of thallium(III) trifluoroacetate, added lithium trifluoroacetate, and arene. [Typical data are listed in Table V for mesitylene.]

presence of added lithium trifluoroacetate revealed a direct correlation between the rate (k_{obsd}) and the concentration of added lithium trifluoroacetate (see Figure 5b). It follows that the inclusion of the trifluoroacetate dissociation (i.e., eq 8) into the Michaelis-Menten dependence described by eq 10 leads to the general expression

$$\frac{1}{k_{\text{obsd}}} = \frac{1}{k_1} + \frac{[\text{LiO}_2\text{CCF}_3]}{k_1 K_1 K_2 [\text{ArCH}_3]} \quad (12)$$

which is independent of the thallium(III) trifluoroacetate concentration.²⁵ The excellent fit of the experimental data to this formulation is shown in Figure 6a, in which all the thallation rates measured at various concentrations of mesitylene, TTFA, and added trifluoroacetate are included on a single line with a correlation coefficient of 0.99. The intercept yields a value of the thallation rate constant as $k_1 = 0.28 \text{ s}^{-1}$, and from the slope a value of 0.20 is obtained for the formation constant product $K_1 K_2$. It is singularly noteworthy that this value of $K_1 K_2$ is the same as that obtained from the Benesi-Hildebrand treatment of the CT absorption data (see Table IV).

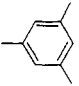
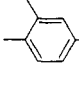
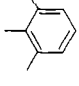
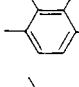
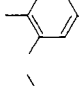
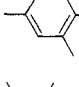
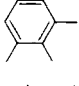
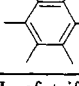
It is important to note in Figure 6b that the same kinetics treatment applies to the side-chain substitution of hexamethylbenzene with TTFA. Despite the difference in the reaction with TTFA, as a comparison of eq 2 and 3 shows, nuclear thallation (R) and side-chain substitution (S) are kinetically indistinguishable insofar as the active thallium(III) species is concerned.

These kinetics results together with the charge-transfer spectral study also provide proof that the thallium(III) species which is active in thallation and that involved in the formation of the EDA

(23) See data in ref 9 and the Experimental Section.

(24) The formulation was originally described by Al-Azzawi and Roberts.⁸ Unfortunately, the discrepancy in the kinetics determined by ^1H NMR and UV-vis spectrophotometry was mistakenly attributed to impurities in TTFA and not to trifluoroacetate dissociation (vide infra).

Table VI. Reactivity of Methylbenzenes in Thallation with $\text{Ti}(\text{O}_2\text{CCF}_3)_2^{+a}$

methylbenzene	$\lambda,^b \text{ nm}$	K_1K_2	$k_1, \text{ s}^{-1}$	$k_1K_2,^c \text{ M}^{-1} \text{ s}^{-1}$	rel rate
	355	0.20	0.28	56	1.00
	360	0.060	0.31	19	0.34, 0.37 ^e
	385	0.061	0.46	28	0.50, 0.57 ^e
	395	0.50	0.31	160	2.8
	395	0.27	0.49	130	2.4
	390	0.21	0.063	13	0.23
	395	1.20	0.25	300	5.4
	330	2.31	0.25	580	10

^aIn 2.0 mL of trifluoroacetic acid containing TTFA ($1-5 \times 10^{-3} \text{ M}$), arenes ($0.010-0.10 \text{ M}$), and LiO_2CCF_3 ($0.010-0.20 \text{ M}$) at 25°C .
^bWavelength used in monitoring the disappearance of the CT band. ^cCalculated from the data in columns 3 and 4 with $K_1 = 1 \times 10^{-3} \text{ M}$. ^dRate of thallation relative to that of mesitylene. ^eDetermined from competition, see text.

complex are the same cationic $\text{Ti}(\text{O}_2\text{CCF}_3)_2^{+}$ resulting from the dissociation of a single trifluoroacetate ligand from TTFA.

(IV) The Reactivity of Various Methylbenzenes in Thallations with $\text{Ti}(\text{O}_2\text{CCF}_3)_2^{+}$. Two independent methods, one based on kinetics and the other on competition, were used to determine the reactivity of various arenes in thallation with TTFA. In the *kinetics method*, the spectral measurement of the CT band described above for mesitylene was extended to the homologous methylbenzenes including other tri- and tetramethylbenzenes as well as penta- and hexamethylbenzene. In every case, first-order kinetics was observed to greater than 90% reaction in the presence of excess arene and added lithium trifluoroacetate. Furthermore, the pseudo-first-order rate constants k_{obsd} followed the relationship in eq 12 with a correlation coefficient of 0.98 or better, for various concentrations of TTFA, methylarene, and lithium trifluoroacetate. The values of the formation constant K_1K_2 and the rate constant k_1 obtained by this procedure are listed in Table VI. It is important to note that the values of the formation constant K_1K_2 for the arene-thallium(III) EDA complex obtained by the kinetics method are the same, to within the experimental uncertainty, as those obtained in Table IV from the Benesi-Hildebrand analysis of the charge-transfer spectral data. The last column lists the second-order rate constant as (k_1K_2) for thallation with $\text{Ti}(\text{O}_2\text{CCF}_3)_2^{+}$.

In the *competition method*, TTFA was treated with a mixture of two methylbenzenes (each in at least 6-fold excess to ensure pseudo-zero-order conditions) and excess LiO_2CCF_3 to maintain the trifluoroacetate concentration constant. The thallated products were analyzed by one of two standard procedures involving either the direct conversion to the aromatic iodide with potassium iodide²⁶ or the isolation of the thallated arene as the chloride complex and

subsequent conversion to the aryl bromide with bromine for quantitation.²⁷ The relative reactivities carried out in this way were independent of the conversion from 30 to 70%, and they are listed in the last column of Table VI. It is noteworthy that the reactivities of the arenes measured by the kinetics and competition methods agree to within the experimental uncertainty of $\pm 10\%$. [Compare the results in columns 5 and 6 in Table VI.] The competition method was not applied to the tetramethylbenzenes and pentamethylbenzene owing to the multiplicity of products obtained in these systems (see Table I).

(V) Kinetic Isotope Effects for Nuclear Thallation and Side-Chain Substitution. Two different types of carbon-hydrogen bonds are cleaved during nuclear thallation and side-chain substitution as described in eq 2 and 3, respectively. The rigorous solution of the kinetics associated with each (as described above) allowed us to examine the deuterium isotope effect both for the pre-equilibrium steps K_1K_2 as well as for the rate constant k_1 . The rate of nuclear thallation of mesitylene was thus compared with that of mesitylene-2,4,6- d_3 , and the rate of side-chain trifluoroacetoxylation of hexamethylbenzene was compared with that of hexamethylbenzene- d_{18} . Comparison of the kinetics results in Tables VI and VII shows no isotope effect for the pre-equilibrium steps, the value of K_1K_2 being essentially independent of deuterium substitution. The same conclusion applies to durene and penta-methylbenzene. Furthermore, the deuterium isotope effect of K_1K_2 determined by an analysis of the kinetics data was the same as that evaluated from the charge-transfer spectra by the Benesi-Hildebrand method. The absence of a primary isotope effect for the pre-equilibrium steps is reasonable for the formation of the π -complex.

The magnitude of the deuterium kinetic isotope effect of the rate constant k_1 for the nuclear thallation of mesitylene is sizable. The value of 7.4 in column 4 of Table VII compares with a slightly

(25) In practice, a 10-fold excess of lithium trifluoroacetate was employed to approximate the zero-order kinetic conditions for trifluoroacetate concentration required in the rigorous application of eq 12.

(26) See ref 1b.

(27) From a procedure described by Olah and co-workers.³

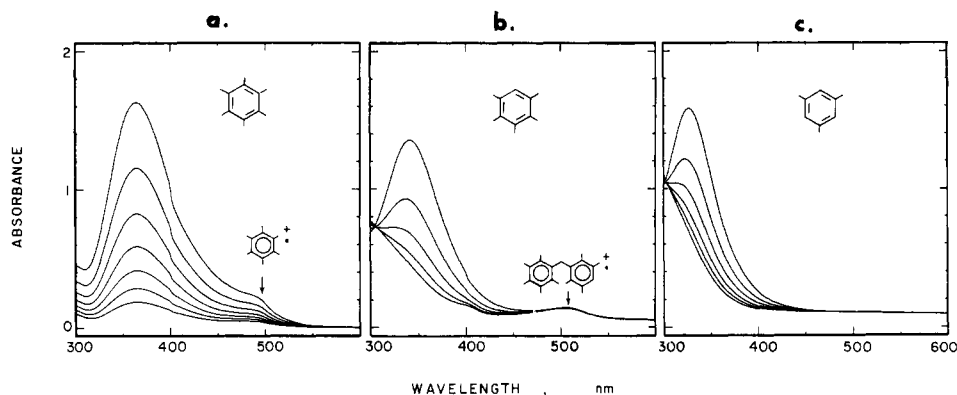
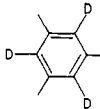
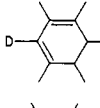
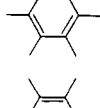
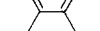


Figure 7. Time-resolved absorption spectra obtained at 5-s intervals during the reaction of TTFA with (a) hexamethylbenzene, (b) pentamethylbenzene and (c) mesitylene in trifluoroacetic acid containing lithium trifluoroacetate. [Note the slight displacement in the absorbance at 400 nm is due to the change of detectors in the spectrophotometer.]

Table VII. Kinetics of Nuclear Thallation and Side-Chain Substitution of Deuteriated Methylbenzenes^a

methylbenzenes	K_1K_2	k, s^{-1}	k_H/k_D^b
	0.28	0.038	7.4
	0.20	0.024	2.6
	0.82	0.099	2.5
	2.4	0.080	3.1

^a Under the same conditions as those in Table VI. ^b Calculated from the kinetic data in column 3 and Table VI, column 4.

smaller value of 3.1 for the side-chain trifluoroacetoxylation of hexamethylbenzene under the same conditions. It is noteworthy that the kinetic isotope effect for durene and pentamethylbenzene which undergo both nuclear thallation as well as side-chain substitutions afford kinetic isotope effects of the same order.

(VI) Observation of Methylbenzene Cation Radicals as Reactive Intermediates. A closer scrutiny of the spectral changes during the thallation of various methylbenzenes by TTFA in trifluoroacetic acid reveals the presence of a minor amount of another transient intermediate. For example, the decay of the CT absorption at 364 nm is clearly observed in the time-resolved absorption spectra in Figure 7a taken at short time intervals during the thallation of hexamethylbenzene. The presence of a minor absorption band at 500 nm is seen to appear immediately upon mixing the components and disappears at a rate similar to the decay of the CT band.

The time-resolved absorption spectra shown in Figure 7b represents the decay of the charge-transfer band of the prehnitene at 342 nm. A minor but more persistent band is clearly discerned at ~510 nm. Absorptions in the region around 500–510 nm can also be observed for the other tetramethylbenzenes as well as pentamethylbenzene. However, no evidence for the presence of a similar absorption band could be observed during the decay of the CT band associated with the mesitylene π -complex shown in Figure 7c.

These electronic absorptions can be readily assigned to small but discrete amounts of arene cation radicals which have been previously observed as an immobilized species in a frozen matrix.²⁸

(28) Badger, B.; Brocklehurst, B. *Trans. Faraday Soc.* **1969**, 65, 2852.

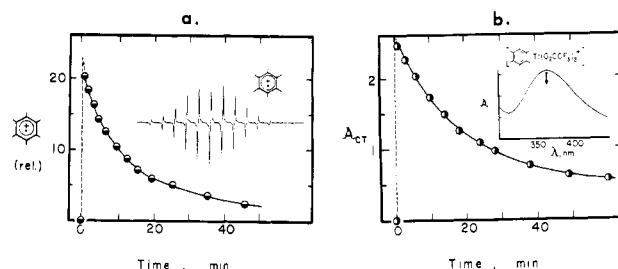
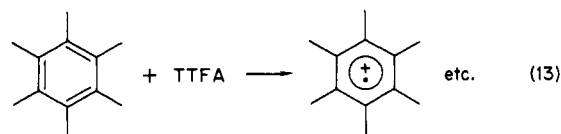


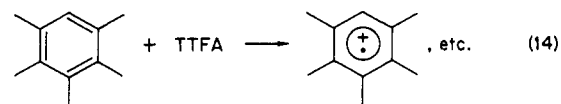
Figure 8. The growth and decay of (a) the hexamethylbenzene cation radical and (b) the charge-transfer absorption band at 364 nm (shown in the insets) during the reaction of 0.025 M hexamethylbenzene, 0.025 M TTFA, and 0.125 M LiO_2CCF_3 at $-10^\circ C$.

Their structural identity has been confirmed by electron spin resonance (ESR) spectroscopy.²⁹ Indeed we find that the ESR spectrum of the hexamethylbenzene cation radical shown in the inset of Figure 8a is observed immediately upon mixing TTFA and hexamethylbenzene in trifluoroacetic acid solutions at $25^\circ C$. The parallel growth and decay of this ESR spectrum with that of the CT band associated with the π -complex shown in Figure 8b is consistent with it being the prime reactive intermediate for the side-chain substitution in eq 3.



[Note that the *absolute* concentration of the hexamethylbenzene cation radical is difficult to determine from its ESR spectrum. The minor absorption band observed at λ_{\max} 500 nm in Figure 7a provides a better indication of its concentration.³⁰]

The series of rather dramatic changes in the ESR spectra derived from pentamethylbenzene are particularly informative. Thus the yellow-orange solution formed immediately upon mixing TTFA with pentamethylbenzene at $-15^\circ C$ affords the ESR spectrum shown in Figure 9a, which coincides with that of the pentamethylbenzene cation radical generated by an independent procedure.^{29,31}



(29) Dessau, R. M.; Shih, S.; Heiba, E. I. *J. Am. Chem. Soc.* **1970**, 92, 412.

(30) We estimate the extinction coefficients of the π -complex at 364 nm and the cation radical at 500 nm to be of the same order of magnitude.

(31) Vincow, G. In "Radical Ions"; Kaiser, E. T., Kevan, L., Eds.; Wiley: New York, 1968.

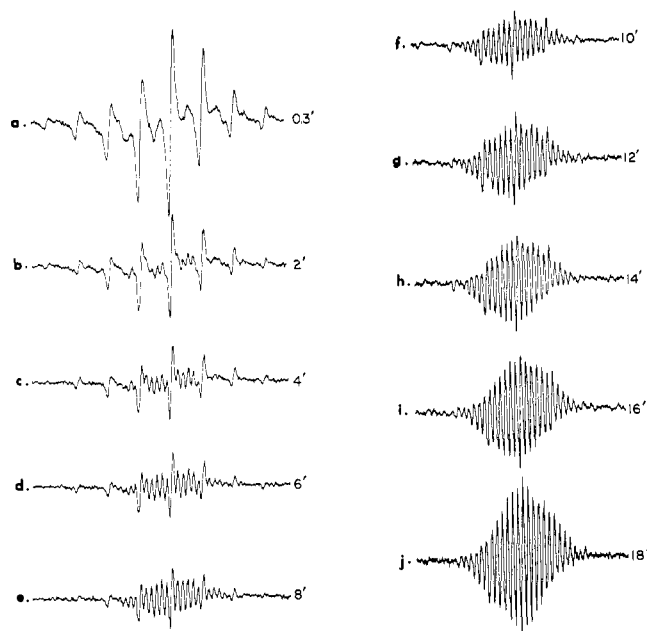


Figure 9. Evolution of the ESR spectra at ~2-min intervals during the reaction of 0.025 M pentamethylbenzene, 0.025 M TTFA, and 0.13 M LiO_2CCF_3 in trifluoroacetic acid at -15°C . All the ESR spectra were measured at approximately the same gain and modulation amplitude.

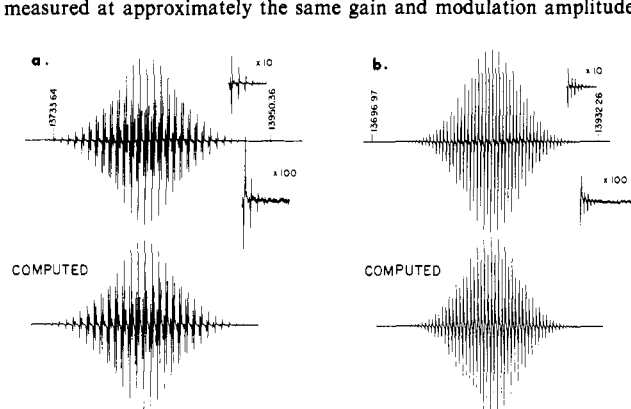
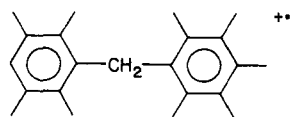


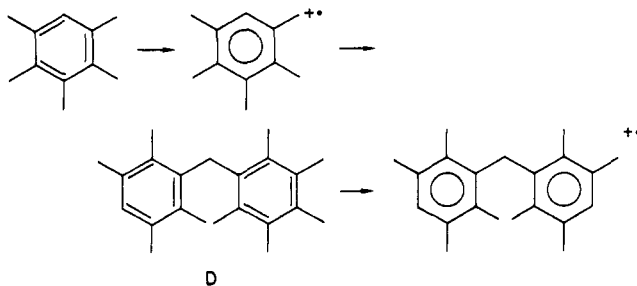
Figure 10. (a) Upper: Resolved ESR spectrum corresponding to that in Figure 9j. Insets show wing lines at 10 and 100 magnification. Lower: Computer simulation with ^1H hyperfine splittings in the text. (b) Upper: Resolved ESR spectrum resulting from the reaction of pentamethylbenzene-*d* with TTFA in $\text{CF}_3\text{CO}_2\text{D}$ under the same conditions as in Figure 9 after equilibration in $\text{CF}_3\text{CO}_2\text{D}$ overnight. Lower: same as in part a but with ^1H splitting replaced by ^2H splitting of 0.84 G.

With time (~20 min), the solution turned deep purple and the ESR spectrum gradually evolved (see Figures 9b–i) to that shown in Figure 9j, which was persistent for several days at room temperature. The same ESR spectrum is shown in Figure 10a at higher resolution. The computer-simulated spectrum below consists of triplets ($a_{2\text{H}} = 5.45$ G) of tridecets ($a_{12\text{H}} = 3.34$ G) of tridecets ($a_{12\text{H}} = 1.67$ G). The paramagnetic species thus contains at least 26 protons with resolvable splittings. We accordingly assign the ESR spectrum in Figure 10a to that of the cation radical derived from the pentamethylbenzene dimer. The structure is presented below to correspond with that of the oxidative dimer (D) isolated from the reaction mixture (see Table I and the Experimental Section).

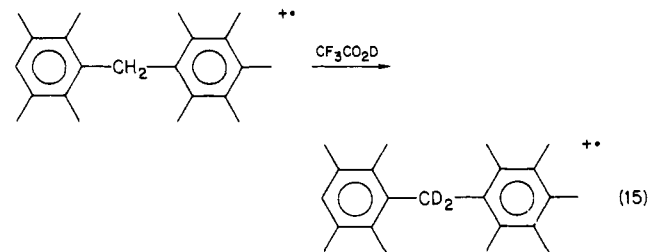


This series of changes in the ESR spectra thus provide compelling support for the prime importance of paramagnetic intermediates during aromatic thallation. Especially clear is the sequence of

electron-transfer events leading to oxidative dimerization (D).



We repeated the foregoing experiment with the monodeuteriated pentamethylbenzene [i.e., $\text{C}_6(\text{CH}_3)_5\text{D}$] in deuteriated trifluoroacetic acid, $\text{CF}_3\text{CO}_2\text{D}$. As expected, the same series of ESR spectra shown in Figure 9a–i were obtained.³² However, a third ESR spectrum shown in Figure 10b was observed when the solution was allowed to equilibrate overnight. The spectrum in Figure 10b corresponds to that in Figure 10a in which the triplet splitting is replaced by a (1:2:3:2:1) quintet arising from a pair of deuteriums with reduced splittings of $a_{2\text{D}} = 0.84$ G, as shown by the comparison with computer-simulated spectrum below. [Note that the reduction by a factor of 6.5 is to within experimental error of the theoretical value.] We conclude that equilibration of the dimer cation radical clearly led to the specific deuterium exchange of only the central methylene protons, i.e.,



The structural details of this interesting cation radical will be elaborated later.

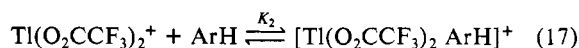
A similar series of complex changes in the ESR spectra observed during the thallation of durene demonstrate that the cation radical as well as that of its oxidative dimer are prime intermediates. However, we could find no evidence for the mesitylene cation radical under the same condition. If it is an intermediate, it must be very short lived.

Discussion

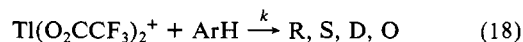
We have found thallium tris(trifluoroacetate) to be readily ionized in trifluoroacetate acid solution according to eq 16, with



a dissociation constant $K_1 \approx 10^{-3}$ M. Quantitative spectrophotometry employing the Benesi–Hildebrand method has established the cationic form of thallium(III) to be the sole species involved in the formation of 1:1 π -complexes with aromatic hydrocarbons, i.e.

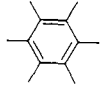
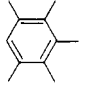
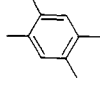
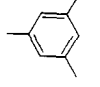
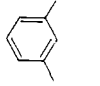



Kinetic studies have also demonstrated that the *same* cationic species is the active form in aromatic thallation leading to nuclear substitution R, side-chain substitution S, oxidative dimerization D, and/or oxidative substitution O, as described in eq 2–5 above, i.e.



Thus spectral analysis and kinetic studies explicitly relegate the undissociated, neutral precursor $\text{Ti}(\text{O}_2\text{CCF}_3)_3$ to the role of an innocent bystander—both in π -complex formation and in aromatic thallation. This allows the concentration of the active thallium(III) species to be readily buffered by added trifluoroacetate ion owing

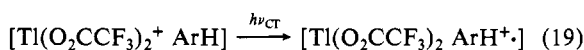
Table VIII. Electron Detachment from Methylbenzenes and the Acidity of Methylbenzene Cation Radicals^a

methylbenzene	I_D , eV	E° , V vs. NHE	pK_a^b
	7.85	1.86	1
	7.92	1.99	-1
	8.07	2.07	-2
	8.42	2.35	-7
	8.56	2.38	-8
	8.82	2.64	-12

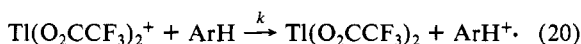
^a Values of I_D in the gas phase and E° in trifluoroacetic acid from ref 34. ^b Estimated value in acetonitrile from ref 41.

to the limiting value of the dissociation constant K_1 .

Aromatic Cation Radicals as Reactive Intermediates Resulting from Electron Transfer. Charge-transfer interactions are integral to π -complex formation (eq 17) and to aromatic thallation (eq 18). Thus the appearance of new spectral bands ($h\nu_{CT}$) arising from the exposure of the cationic thallium(III) acceptor to various aromatic donors in Table II is, according to Mulliken theory,^{16,17} associated with the vertical transition leading to electron transfer within the π -complex,³³ i.e.



Analogously, the ESR observation of aromatic cation radicals (formed as intermediates during the aromatic thallation of hexamethylbenzene, pentamethylbenzene and durene) derives from a bimolecular process involving electron transfer, i.e.



In both cases the overall effect is for the aromatic hydrocarbon to suffer one-electron loss to the cationic thallium(III) species acting as an oxidant. As such, the energetics of electron detachment are dependent on the ionization potential I_D and the reversible oxidation potential E° of the aromatic compound in the gas phase and in solution, respectively.³⁴ These values are summarized in Table VIII for the aromatic hydrocarbons of interest to this study.

The kinetics of electron transfer in eq 20 is related directly to the disappearance of π -complex formed in eq 17 in the following manner. The change in the concentration of the π -complex derived from hexamethylbenzene and $Ti(O_2CCF_3)_2^+$ can be followed by the decay of its CT absorption band at 330 nm (see Table II). Similarly, the electron transfer in eq 20 leads to the hexamethylbenzene cation radical which is readily measured from its

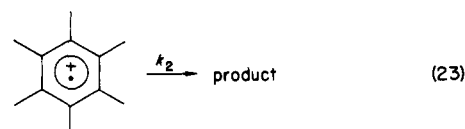
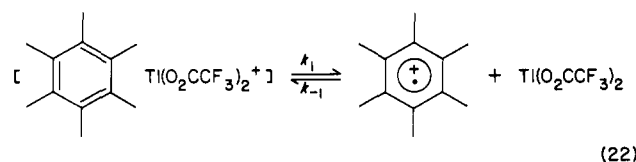
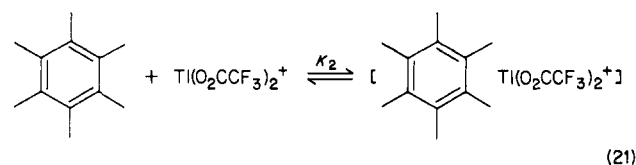
(32) Since the hyperfine splitting of the ring proton on the ring is too small to measure (<0.1 G), the ESR spectra of $C_6(CH_3)_5H^{\cdot+}$ and $C_6(CH_3)_5D^{\cdot+}$ are the same experimentally.

(33) For a recent experimental verification of such a CT process in the anthracene-tetracyanoethylene complex, see: Hilinski, E. F.; Masnovi, J. M.; Amatore, C.; Kochi, J. K.; Rentzepis, P. M. *J. Am. Chem. Soc.* **1983**, *105*, 6167.

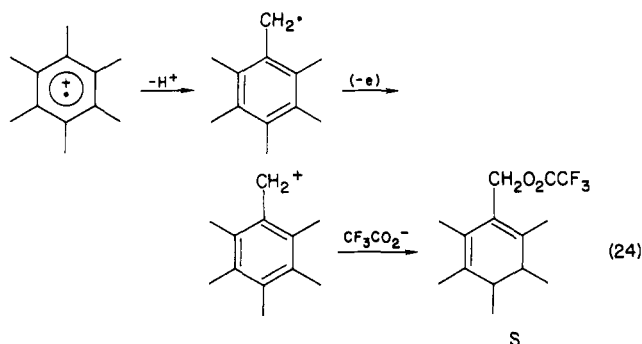
(34) Howell, J. O.; Goncalves, J.; Amatore, C.; Klasinc, L.; Wightman, R. M.; Kochi, J. K. *J. Am. Chem. Soc.* **1984**, *106*, 3968.

ESR spectrum (see Figure 8). The direct relationship between the steady-state concentrations of these two intermediates shown in Figure 11 follows from the mechanism in Scheme II with the rate constants $k_2 \ll k_{-1}$.

Scheme II



In other words, the steady-state concentration of the aromatic cation radical is dominated by the rate of back-electron transfer (k_{-1}) in eq 22, that is faster than the follow-up reaction (k_2) in eq 23. Such reactions of hexamethylbenzene cation radicals have been identified in various chemical and electrochemical oxidations of hexamethylbenzene.³⁶⁻³⁹ Thus hexamethylbenzene cation radicals have been shown to afford side-chain substitution products (S) via sequential proton and electron loss,⁴⁰ e.g.



Indeed the deuterium kinetic isotope effect of 3.1 for the side-chain substitution of hexamethylbenzene (see Table VII) is associated with proton loss in eq 24.⁴¹

The other aromatic products such as D and O are also characteristic of a wide variety of analogous cation radicals generated by either chemical or electrochemical oxidations of aromatic hydrocarbons.^{38,39} For example, the dimeric aromatic hydrocarbons (D) are known to result from methylbenzene cation radicals via the attack of the benzylic cation on the parent arene,⁴² e.g.

(35) The rate constants k_1 and k_2 are kinetically equivalent insofar as they both involve diffusive processes of the reactive pair.

(36) Beletskaya, I. P.; Makhon'kov, D. I. *Russ. Chem. Rev. (Engl. Transl.)* **1981**, *50*, 534.

(37) Ross, S. D.; Finkelstein, M.; Rudd, E. J. "Anodic Oxidation"; Academic Press: New York, 1975.

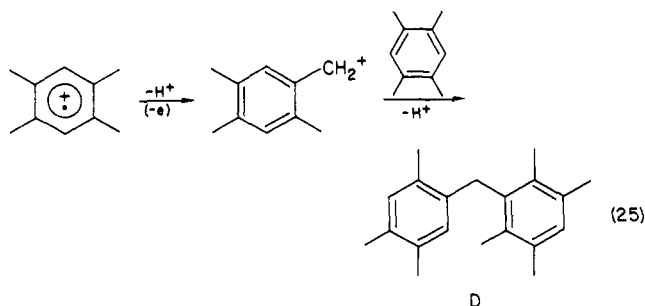
(38) Yoshida, K. "Electrooxidation in Organic Chemistry"; Wiley: New York, 1984.

(39) Bard, A. J.; Ledwith, A.; Shine, H. J. *Adv. Phys. Org. Chem.* **1976**, *13*, 155.

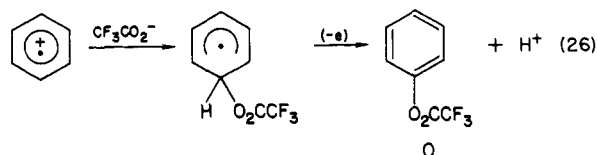
(40) Schlesener, C. J.; Amatore, C.; Kochi, J. K. *J. Am. Chem. Soc.* **1984**, *106*, 3567.

(41) Compare with the following: Schlesener, C. J.; Amatore, C.; Kochi, J. K. *J. Am. Chem. Soc.*, in press.

(42) Parker, V. D.; Adams, R. N. *Tetrahedron Lett.* **1969**, 1721. See also ref 38, pp 133 ff.

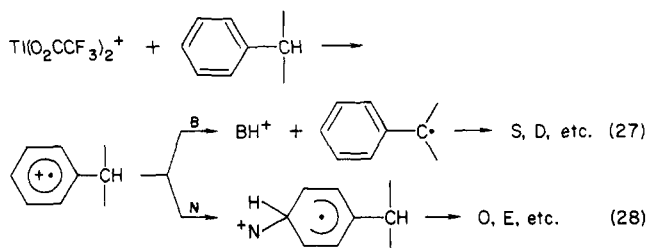


Furthermore, the direct addition to the aromatic ring of electron-deficient cation radicals by various nucleophiles can lead to oxidative substitution (O),⁴³ e.g.



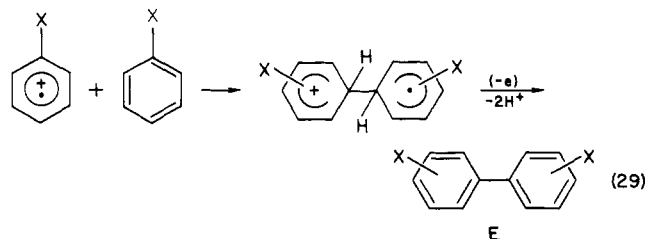
Since each of the aromatic products S, D, and O derive from a common cation radical precursor, it is important to delineate the pathways by which they are differentiated. The general problem is basically described by the reactivity of electron-deficient cation radicals toward bases B and nucleophiles N in the following formulation.

Scheme III



According to this generalized scheme, side-chain substitution (S) and dimer formation (D) are dependent on the acidity of methylbenzene cation radicals. [The pK_a values of various $ArCH_3^+$ have been recently estimated and are included in Table VIII.] The subsequent electron detachment from benzylic radicals (as in eq 24) is known to be facile,⁴⁴ and the resulting benzylic cation also reacts rapidly with anions such as trifluoroacetate and aromatic donors to afford S and D, respectively.⁴⁵ Thus side-chain substitution and dimer formation are intrinsically controlled by the rate of proton loss from the aromatic cation radical in eq 27.

Oxidative substitution (O) on the other hand stems from the nucleophilic attack directly on the aromatic ring of the cation radical. Such an addition step will be rate limiting since the subsequent oxidation of the adduct radical and proton loss (as in eq 26) is likely to be rapid. This formulation also includes electron-rich aromatic compounds as nucleophiles which are capable of adding to the cation radical to afford biaryls (E), e.g.



where the substituent X is commonly an electron-releasing alkoxy group.⁴⁶ In this regard, the oxidative dimerization of aryl ethers and related electron-rich arenes by TTFA^{2,47} is related to the same process induced by electrochemical oxidation^{37,38} and by various metal complexes known to effect one-electron oxidation.³⁶

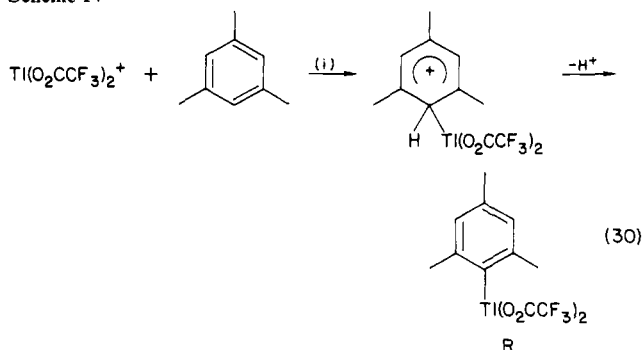
The dichotomy in Scheme III basically represents the competition between (a) proton transfer from a carbon center in eq 27 and (b) nucleophilic addition to the ring of this electron-deficient intermediate in eq 28.⁴⁸ Several factors have been identified in this competition.³⁶⁻³⁹ First, the acidity of the methylbenzene cation radical generally increases monotonically with the number of methyl substituents (see Table VIII).⁴¹ Second, the rate of deprotonation from $ArCH_3^+$ follows the base strength to accord with the Brønsted relationship⁴¹—as a result, trifluoroacetate is more effective than trifluoroacetic acid which in turn is much more effective than an aromatic donor. Third, since the direct attack on the ring of an aromatic cation radical increases with nucleophilic strength, the effectiveness of an aromatic donor (cf. eq 29) is not highly distinguished from that of trifluoroacetic acid (cf. eq 26). These factors taken together provide an adequate rationale for aromatic cation radicals as the reactive intermediate which is subsequently partitioned among the different products S, D, and O according to the nature of the aromatic donor in Table I.

Nuclear Thallation with the Cationic Thallium(III) Electrophile.

Nuclear thallation R occurs with the methylbenzenes in Table I whenever there is an unsubstituted position in the ring—hexamethylbenzene thus being the only arene in which this process is not possible. Kinetic studies have established the cationic $Tl(O_2CCF_3)_2^+$ to be the active thallium(III) species, as it is in the electron-transfer processes described above. However, there is a distinction between nuclear thallation (leading to R) and electron transfer (leading to S, D, and/or O) which is dependent on the degree of methyl substitution. Thus the extent of nuclear thallation in Table I falls off monotonically in the order mesitylene ($\sim 100\%$) > durene ($\sim 50\%$) > and pentamethylbenzene ($\sim 25\%$)—with a concomitant increase in the proportion of products S, D, and O derived from the aromatic cation radical.

Let us now consider the mechanism of nuclear thallation in the light of the competing electron-transfer process described in Scheme III. If nuclear thallation proceeds via an electrophilic mechanism (as is commonly considered to be the case), the sequence of steps leading from an arene such as mesitylene and the active, cationic thallium(III) electrophile would be:

Scheme IV



The activation process for nuclear thallation according to Scheme IV is represented as an electrophilic attack by $Tl(O_2CCF_3)_2^+$ on the aromatic ring to form the Wheland intermediate in step i. Such a mechanism involves the creation of the new carbon-thallium bond in a single, concerted step. This overall two-electron

(43) See ref 13.

(44) Rollick, K. L.; Kochi, J. K. *J. Am. Chem. Soc.* **1982**, *104*, 1319.

(45) For example, see: Lowry, T. H.; Richardson, K. S. "Mechanism and Theory in Organic Chemistry"; 2nd ed.; Harper and Row: New York, 1981; Chapter 4.

(46) See ref 38 and 39 for other examples.

(47) Taylor, E. C.; Andrade, J. G.; Rall, G. J. H.; Turchi, I. J.; Steliou, K.; Jagdmann, G. E.; McKillop, A. *J. Am. Chem. Soc.* **1981**, *103*, 6856; *J. Org. Chem.* **1981**, *46*, 3078.

(48) For a detailed discussion of this competition, see: Schlesener, C. J.; Kochi, J. K. *J. Org. Chem.* **1984**, *49*, 3142.

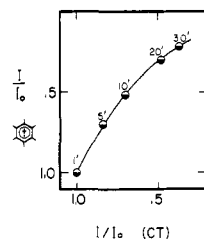


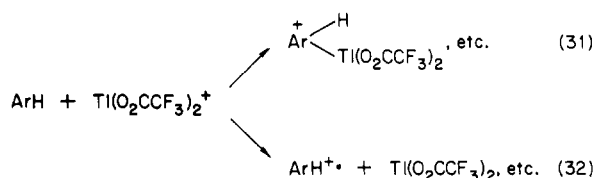
Figure 11. Comparative rates of disappearance of the hexamethylbenzene cation radical and the hexamethylbenzene-thallium(III) π -complex, as indicated by the changes in the intensity of the ESR spectrum and the charge-transfer absorbance, respectively.

or ionic transformation contrasts with that presented in Scheme III in which the same cationic $\text{Ti}(\text{O}_2\text{CCF}_3)_2^+$ participates in a one-electron reduction. In other words, the basic dichotomy between nuclear thallation and electron transfer is the capacity of the active thallium(III) species to undergo a two-electron or a one-electron reduction, respectively.

Electrophilic vs. Electron-Transfer Pathways—Separate or Common Transition States? Viewed from a slightly different perspective, the interaction of aromatic compounds with TTFA represents a system in which ionic and free radical processes are closely juxtaposed. This situation is strongly underscored by the results of the kinetics data presented in Table VI. Thus the reactivity of mesitylene toward nuclear substitution is essentially of the same order of magnitude as the reactivity of hexamethylbenzene to electron transfer, as indicated by these magnitudes of the second-order rate constants listed in Table VI. Furthermore, the reactivities of durene and pentamethylbenzene, in which both the electrophilic and electron-transfer processes occur simultaneously, are also of comparable magnitudes. Thus the reactivity of a given aromatic hydrocarbon toward $\text{Ti}(\text{O}_2\text{CCF}_3)_2^+$ provides no clear-cut distinction between the nature of the transition state for the two-electron electrophilic process and that for a one-electron transfer process.

There are essentially two ways in which this paradox can be resolved. First it is possible that electrophilic nuclear thallation and one-electron transfer are simply *competing pathways* which proceed via different activated complexes.

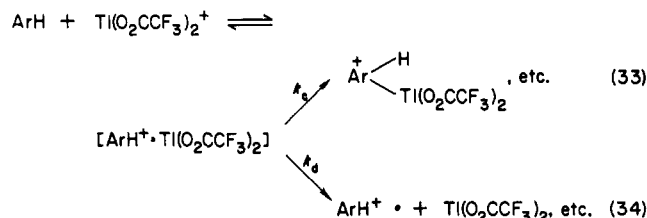
Scheme V



If so, those factors related to the donor properties of aromatic compounds such as π -complex formation, charge-transfer excitation, ionization and oxidation potentials, rates, etc., are too common to both to allow any kinetics distinction between these independent pathways. Moreover, their strong dependence on the unique character of the active thallium(III) species, namely the cationic $\text{Ti}(\text{O}_2\text{CCF}_3)_2^+$, further obscures any difference in their transition states. This mechanism thus recognizes two such apparently dissimilar processes as electrophilic thallation and electron transfer to be remarkably alike. Such kindred transition states can be theoretically accommodated within the valence-bond approach to electrophile-nucleophile reactivity, as described by Pross and Shaik.⁴⁹

The second mechanistic alternative is that electrophilic nuclear thallation and one-electron transfer proceed via a *common intermediate*, viz., the aromatic cation radical, which is subsequently partitioned in a rapid follow-up step, i.e.

Scheme VI



According to Scheme VI, the two principal pathways are differentiated during the competition between the cage collapse (k_c) and the diffusive separation (k_d) of the reactive pair in eq 33 and 34, respectively. The ESR observation of the cation radical from hexamethylbenzene as a dominant intermediate (see Figure 8) would then be consistent with the unavailability of cage collapse for this arene, i.e., $k_d \gg k_c$. Likewise, the inability to observe the cation radical from mesitylene would be attributed to a rate of collapse to the Wheland intermediate which is substantially faster than diffusive separation, i.e., $k_c \gg k_d$. The mixture of products derived from electrophilic thallation and electron transfer with durene and pentamethylbenzene would represent an intermediate situation in which $k_c \sim k_d$. However, there is an important caveat to this description of the competition. Thus the evaluation of the deuterium kinetic isotope effects in Table VII indicates that the subsequent proton loss from both the Wheland intermediate and the cation radical intermediate must be taken explicitly into account in the kinetics. Thus the overall reactivity and products derived from an aromatic hydrocarbon and TTFA will depend on (a) its donor properties as measured by the magnitudes of I_D , E° , or $h\nu_{CT}$, (b) the properties of the aromatic cation radical relative to further reactions [cf. eq 24–26 and 29], and (c) the rate of proton loss from the reactive intermediates $\text{Ar}(\text{H})\text{Ti}(\text{O}_2\text{CCF}_3)_2^+$ and $\text{ArH}^+ \cdot$ in eq 33 and 34, respectively.

Conclusions

Concurrent electrophilic and electron-transfer pathways have been demonstrated for the interaction of a series of homologous methylbenzenes [ArCH_3] with thallium(III) trifluoroacetate or TTFA in trifluoroacetic acid. The pre-equilibrium formation of a 1:1 π -complex is common to both, and it is quantitatively assessed by the Benesi-Hildebrand analysis of the transient charge-transfer bands. The cationic $\text{Ti}(\text{O}_2\text{CCF}_3)_2^+$, which is formed from TTFA by dissociation of a single trifluoroacetate ligand with $K \approx 1 \times 10^{-3}$ M, is the active thallium(III) species involved in π -complex formation as well as in the activation process for the electrophilic and electron-transfer reactions. The experimental dissection of the complex kinetics shows that the second-order rate constants leading to electrophilic aromatic substitution and that leading to electron transfer are comparable. Such a close competition identifies the mechanistic conundrum of distinguishing between two-electron (concerted) and one-electron (stepwise) pathways which proceed via rate-limiting transition states which are not highly differentiated. In a following report we will present experimental approaches to help resolve this challenging problem, which is pervasive in organic chemistry.

Experimental Section

Materials. The aromatic hydrocarbons were obtained from commercial sources and repurified as follows. Hexamethylbenzene, pentamethylbenzene, and durene (Aldrich Chem. Co.) were recrystallized from ethanol and sublimed. Prehnitene and mesitylene (Aldrich Chem. Co.) as well as isodurene and pseudocumene (Wiley Chem. Co.) were refluxed over sodium and distilled under reduced pressure. Hemimellitene (Aldrich) was converted to the crystalline sulfonic acid derivative which was purified and subsequently hydrolyzed.⁵⁰ The isomeric purity of each hydrocarbon was established by gas-chromatographic analysis on a Hewlett-Packard 5790 chromatograph equipped with a 12-m capillary column coated with cross-linked methylsilicone.

(49) For a review, see: Pross, A.; Shaik, S. S. *Acc. Chem. Res.* **1983**, *16*, 363. Charge-transfer contributions are implicit in the valence-bond configuration-mixing model.

(50) Perrin, D. D.; Armarego, W. L. F.; Perrin, D. R. "Purification of Laboratory Chemicals"; Pergamon Press: Elmsford, New York, 1966.

Hexamethylbenzene- d_{18} (Merck) was received as a gift from Dr. A. E. Nader (DuPont) and used as such. The ring-deuteriated pentamethylbenzene- d_1 , durene-2,5- d_2 , and mesitylene-2,4,6- d_3 were prepared by proton exchange in trifluoroacetic acid. In a typical procedure, mesitylene (2.0 mL) was added to a mixture of trifluoroacetic anhydride (5 mL) and deuterium oxide (5 mL), and the solution was refluxed overnight. The reaction mixture was extracted with methylene chloride, and the extract was neutralized and dried with Na_2CO_3 . The solvent was removed in vacuo, and the mesitylene recovered after one exchange was 93% complete, as estimated by integration of ^1H NMR resonance of the aromatic proton relative to that of the methyl groups. The exchange procedure was repeated, and the recovered mesitylene upon distillation showed no aromatic protons (<1%) in the ^1H NMR spectrum. The deuteriated mesitylene was further analyzed on a Hewlett-Packard Model 5992 gas chromatograph-mass spectrometer. The mass spectral cracking pattern of mesitylene- d_3 at 70 eV consisted of m/z (%) 108 (100), 122 (14), 123 (53), 124 (6), which compared with that of mesitylene, 105 (100), 119 (10), 120 (42), 121 (4). Pentamethylbenzene- d_1 and durene- d_2 were prepared by a similar procedure. Each arene which was isolated after two exchanges was sublimed in vacuo and showed >99% deuteration of the aromatic protons.

4-Iodo-1,3-dimethylbenzene (Pfaltz and Bauer Co.) was used as received. Iodomesitylene, iododurene, and iodopentamethylbenzene were prepared by a procedure described by Sugiyama.⁵¹ Thallium(III) trifluoroacetate (TTFA) was prepared from thallic oxide (Asarco) in a mixture of trifluoroacetic acid containing 2 mol % water.⁵² It was recrystallized from a mixture of trifluoroacetic acid and trifluoroacetic anhydride. Lithium trifluoroacetate (Alfa) was repurified by recrystallization from a mixture of trifluoroacetic acid and its anhydride. In order to prevent exposure to moisture, all manipulations were carried out with use of Schlenkware techniques.

Charge-Transfer Spectral Measurements. The UV-vis absorption spectra were measured on a Hewlett-Packard 8450A diode array spectrometer capable of 0.1-s time resolution and a repetition rate of 1 s. Temperature control of $\pm 0.1^\circ\text{C}$ was maintained by a Hewlett-Packard 89100 A thermostatic accessory. In a typical measurement, either a 10-, 2-, or 1-mm quartz cuvette equipped with sidearm and Schlenk adaptor was flame dried in vacuo and filled with dry argon. Aliquots of 0.01 M TTFA in trifluoroacetic acid (0.20 mL) and 0.1 M lithium trifluoroacetate in the same solvent (0.20 mL) were transferred together with 1.50 mL of trifluoroacetic acid to the main compartment with the aid of air-tight hypodermic syringes equipped with platinum needles under argon. An aliquot of 0.20 M mesitylene dissolved in trifluoroacetic acid (0.10 mL) was carefully loaded into the sidearm using the same technique. The cuvette was thermally equilibrated, and the reaction was initiated by a rapid shaking of the contents (<2 s).

The charge-transfer absorptions were measured at various concentrations of TTFA (typically $1-5 \times 10^{-3}$ M), arenes (1×10^{-2} to 2×10^{-1} M), and lithium trifluoroacetate (0–0.4 M) to ensure homogeneity in the band shapes and constancy of the maximum λ_{max} . The spectra were measured repetitively at 2-s intervals, and the initial absorbance \mathcal{A}_0 was obtained by extrapolation to zero time. The formation constant associated with the charge-transfer band was obtained by plotting the ratio $[\text{TTFA}]/\mathcal{A}$ as a function of $[\text{LiO}_2\text{CCF}_3]/[\text{ArCH}_3]$ according to the Benesi-Hildebrand expression:

$$[\text{TTFA}]/\mathcal{A} = 1/\epsilon + (K_1 + [\text{LiO}_2\text{CCF}_3])/(K_1 K_2 \epsilon [\text{ArCH}_3])$$

Since the spectral measurements were all carried out with excess lithium trifluoroacetate (i.e., $[\text{LiO}_2\text{CCF}_3] \gg K_1$), the plots yielded lines with intercepts corresponding to ϵ^{-1} and slopes of $(K_1 K_2 \epsilon)^{-1}$.

Product Identification and Analysis. All thermal reactions of arenes with TTFA were carried out in a Schlenk flask under an inert argon atmosphere and shielded from direct room light. Stock solutions of TTFA (0.10 M), lithium trifluoroacetate (0.10 M), and the appropriate arene (0.10 M) were prepared in degassed trifluoroacetic acid [3.0 mL]. Dodecane was added as an internal standard since control experiments showed that it had no effect on the thallation reactions. The colors, formed immediately upon mixing the components, varied from yellow (mesitylene) to orange (hexamethylbenzene). After 1–3 h, the reactions were quenched with 2.0 mL of aqueous potassium iodide (1.0 M). The mixture containing a massive yellow precipitate was extracted with 2 mL of methylene chloride. Control experiments with authentic arylthallium bis(trifluoroacetate) established that this procedure led to quantitative yields of the corresponding aryl iodide.⁹

The aryl iodides were each identified and their amount quantified by quantitative gas chromatography in comparison with that of an authentic sample. The mass spectra of aryl iodides show a characteristic frag-

mentation of the aryl-iodine bond yielding Ar^+ as the major fragment ions, in addition to relatively minor amounts of the parent ion ArI^+ and I^+ (m/z 127, 128).

The ester formed from hexamethylbenzene was identical with that of an authentic sample prepared by anodic oxidation.⁵³ The ^1H NMR spectrum of pentamethylbenzyl trifluoroacetate showed singlet resonances at δ 5.45 (2 H), 2.22 (9 H), and 2.17 (6 H). The mass spectrum showed the parent ion at m/z 274, as well as a characteristic fragmentation pattern for a benzylic trifluoroacetate, viz., m/z (%) 69 (15), 77 (12), 91 (22), 105 (16), 115 (13), 119 (11), 129 (11), 131 (12), 145 (25), 160 (100), 161 (86), 162 (11), 274 (13).

The thallation of pentamethylbenzene with TTFA and no added LiO_2CCF_3 under similar conditions yielded two principal products in addition to the aryl iodide. The product, pentamethylphenyl trifluoroacetate, was the same as that previously isolated and characterized.⁵⁴ The ^1H NMR spectrum consisted of two singlet resonances at δ 2.22 (9 H) and 2.08 (6 H), and no observable aromatic proton resonance. The mass spectrum showed no parent ion at m/z 260, but the fragments corresponding to $(\text{CH}_3)_5\text{C}_6\text{O}^+$ at 163, $(\text{CH}_3)_5\text{C}_6^+$ at 147, CF_3^+ at 69 and CF_3CO^+ at 97 are characteristic of aryl trifluoroacetates. For $(\text{CH}_3)_5\text{C}_6\text{O}_2\text{CCF}_3$, m/z (%) 35 (34), 39 (59), 40 (12), 41 (52), 43 (17), 47 (20), 48 (11), 49 (74), 50 (20), 51 (38), 53 (31), 63 (11), 65 (18), 69 (100), 77 (19), 79 (15), 84 (10), 91 (33), 97 (12), 105 (31), 107 (10), 115 (11), 117 (12), 119 (26), 131 (11), 146 (19), 147 (33), 163 (14). The other product corresponded to the dimeric hydrocarbon $\text{C}_{22}\text{H}_{30}$ with the parent peak in the mass spectrum m/z 294. The base peak at m/z 160 derives from the fragmentation at a benzylic bond corresponding to the structure $(\text{CH}_3)_5\text{C}_6\text{CH}_2\text{C}_6(\text{CH}_3)_4\text{H}$, i.e., m/z (%) 91 (19), 105 (12), 115 (12), 117 (13), 131 (15), 145 (16), 146 (82), 147 (24), 160 (100), 161 (16), 279 (16), 294 (22). The gas-chromatographic retention time of this product also corresponded to that of the dimeric hydrocarbon, which was quantified relative to an eicosane internal standard. The assignment of the tetramethylphenyl moiety in the dimer was based on the ESR spectrum of the cation radical (vide infra), but it must be established by independent synthesis now in progress.⁵⁵

The thallation of durene affords iododurene and the dimeric hydrocarbon as the major products. A minor product tentatively identified as a trifluoroacetate ester was also present, but in amounts too small to characterize thoroughly. The mass spectrum of the dimer showed the parent peak at m/z 266 and a base peak at 146 characteristic of the fragmentation of a benzylic bond in $(\text{CH}_3)_4\text{C}_6\text{HCH}_2\text{C}_6(\text{CH}_3)_3\text{H}_2$, i.e., m/z (%) 77 (13), 91 (24), 105 (17), 115 (17), 117 (21), 131 (22), 132 (51), 133 (25), 146 (100), 147 (15), 251 (13), 266 (22). The amount of dimer formed was analyzed by gas chromatography with eicosane as the internal standard.

The thallation product derived from mesitylene is readily determined from its ^1H NMR spectrum.⁹ The product $(\text{CH}_3)_3\text{C}_6\text{H}_2\text{Ti}(\text{O}_2\text{CCF}_3)_2$ could be readily isolated as a colorless crystalline solid in rather pure form simply by removal of the solvent in vacuo. It was converted to iodo-mesitylene in quantitative yields with potassium iodide.

Kinetics Measurements. The absolute rates of reaction between TTFA and the various arenes were followed spectrophotometrically by monitoring the disappearance of the charge-transfer absorption bands at selected wavelengths as indicated in the tables. The technique was essentially the same as that described above. Unless indicated otherwise, all the reactions were carried out in the dark at 25°C , and their course was followed to >90% completion. In a typical situation, aliquots of 0.01 M TTFA (0.20 mL), 0.10 M lithium trifluoroacetate (0.20 mL), 0.20 M arene (0.10 mL), and 1.5 mL trifluoroacetic acid were employed. The pseudo-first-order rate constant k_{obsd} was obtained from the least-squares evaluation of the slope of the absorbance change $\ln(\mathcal{A}_t - \mathcal{A}_\infty)$ with time where \mathcal{A}_t and \mathcal{A}_∞ are the absorbances of the CT band at time t and final time, respectively. In all cases, linearity in the pseudo-first-order plots was attained with a correlation coefficient of 0.985 or better. The kinetics were carried out at various concentrations of the arenes while always maintaining an excess of lithium trifluoroacetate.

The relative rates of reaction of various arenes with TTFA were determined by a competition method similar to that described by Olah, Stock, and co-workers.^{3,7} Thallations were carried out in trifluoroacetate acid solutions containing a large excess of LiO_2CCF_3 in order to maintain a constant level of trifluoroacetate. The relative amounts of thallated arenes were determined by analyzing the aryl iodide formed upon iodolysis (vide supra), by gas chromatography with a Hewlett-Packard 5790 chromatograph equipped with a 12-m capillary column coated with cross-linked methylsilicone. In a typical experiment, 1,2,4-trimethylbenzene (0.410 g, 3.42 mmol) and mesitylene (0.077 g, 0.65 mmol) were

(51) Sugiyama, T. *Bull. Chem. Soc. Jpn.* **1981**, *54*, 2847.

(52) Cf.: Kochi, J. K.; Bethea, T. W., III *J. Org. Chem.* **1968**, *33*, 75.

(53) Chen, K. S., unpublished observations, and ref 46 and 10.

(54) Lau, W., to be published.

(55) Katta, V., unpublished results.

dissolved in 4 mL of trifluoroacetic acid containing 0.50 mmol of LiO_2CCF_3 . The mixture was equilibrated at 25 °C, and 1 mL of 0.1 M TTFA in trifluoroacetic acid was added. After standing for 5–15 min shielded from light, the mixture was treated with 2 mL of 1.0 M aqueous KI whereupon the solution immediately turned dark, followed by the formation of a large amount of yellow precipitate. After 15 min, the mixture was extracted with 2.0 mL of methylene chloride. Analysis of the unreacted arene and aryl iodide by gas chromatography yielded the relative reactivities as $k(\text{mesitylene})/k(\text{pseudocumene}) = [\text{mesityl iodide}]/[\text{pseudocumene}]/[\text{pseudocumyl iodide}]/[\text{mesitylene}] = 2.7$. The ratio was confirmed by carrying out an indirect competition of mesitylene and pseudocumene against *m*-xylene. Thus these relative reactivities of 11.0 and 3.7, respectively, correspond to an indirect competition of 3.0 which is in agreement with the value obtained from the direct competition. These relative reactivities also agree with those obtained from the kinetic measurements in Table VI.

Electron Spin Resonance Spectral Measurements. The samples for ESR spectroscopy were prepared in 2-mm (i.d.) Pyrex tubes sealed in vacuo. In a typical procedure a stock solution consisting of 0.050 M TTFA and 0.25 M LiO_2CCF_3 and one consisting of 0.050 M hexamethylbenzene were prepared separately. Each was degassed by three freeze-pump-thaw cycles and protected from moisture and air under an argon atmosphere. The sample tube was connected to a Schlenk adaptor, flame dried in vacuo, and filled with argon. A 0.2-mL aliquot of the TTFA was transferred to the tube under argon with the aid of a hypodermic syringe and platinum needle. The contents were frozen and an 0.2-mL aliquot of the hexamethylbenzene solution added under the same conditions and frozen on top of the TTFA layer. The two separate layers were allowed to melt quickly in a bath at -20 °C, mixed, and inserted

into the ESR cavity maintained at -10 °C by a flow of cold nitrogen. The spectra were recorded on a Varian E112 spectrometer equipped with a Harvey-Wells G502 gaussmeter and Hewlett-Packard Model 5248L electronic counter and model 5255A frequency converter.

Acknowledgment. We thank Dr. C. Amatore for help with the kinetics treatment and the National Science Foundation for financial support.

Registry No. TTFA, 23586-53-0; $[(\text{CH}_3)_6\text{C}_6\text{Ti}(\text{O}_2\text{CCF}_3)_3]$, 92397-33-6; $[(\text{C}_2\text{H}_5)_6\text{C}_6\text{Ti}(\text{O}_2\text{CCF}_3)_3]$, 92397-34-7; $[(\text{CH}_3)_5\text{C}_6\text{HTl}(\text{O}_2\text{CCF}_3)_3]$, 92397-35-8; $[1,2,3,4-(\text{CH}_3)_4\text{C}_6\text{H}_2\text{Ti}(\text{O}_2\text{CCF}_3)_3]$, 92397-36-9; $[1,2,3,5-(\text{CH}_3)_4\text{C}_6\text{H}_2\text{Ti}(\text{O}_2\text{CCF}_3)_3]$, 92397-37-0; $[1,2,4,5-(\text{CH}_3)_4\text{C}_6\text{H}_2\text{Ti}(\text{O}_2\text{CCF}_3)_3]$, 92397-38-1; $[1,2,3-(\text{CH}_3)_3\text{C}_6\text{H}_3\text{Ti}(\text{O}_2\text{CCF}_3)_3]$, 92397-39-2; $[1,2,4-(\text{CH}_3)_3\text{C}_6\text{H}_3\text{Ti}(\text{O}_2\text{CCF}_3)_3]$, 92397-40-5; $[1,3,5-(\text{CH}_3)_3\text{C}_6\text{H}_3\text{Ti}(\text{O}_2\text{CCF}_3)_3]$, 92397-41-6; $[1,2-(\text{CH}_3)_2\text{C}_6\text{H}_4\text{Ti}(\text{O}_2\text{CCF}_3)_3]$, 92397-42-7; $[1,3-(\text{CH}_3)_2\text{C}_6\text{H}_4\text{Ti}(\text{O}_2\text{CCF}_3)_3]$, 92397-43-8; $[1,4-(\text{CH}_3)_2\text{C}_6\text{H}_4\text{Ti}(\text{O}_2\text{CCF}_3)_3]$, 92420-19-4; $[t\text{-C}_4\text{H}_9\text{C}_6\text{H}_3\text{Ti}(\text{O}_2\text{CCF}_3)_3]$, 92397-44-9; $[i\text{-C}_3\text{H}_7\text{C}_6\text{H}_5\text{Ti}(\text{O}_2\text{CCF}_3)_3]$, 92397-45-0; $[\text{C}_2\text{H}_5\text{C}_6\text{H}_5\text{Ti}(\text{O}_2\text{CCF}_3)_3]$, 92397-46-1; $[\text{CH}_3\text{C}_6\text{H}_5\text{Ti}(\text{O}_2\text{CCF}_3)_3]$, 92397-47-2; $[\text{C}_6\text{H}_6\text{Ti}(\text{O}_2\text{CCF}_3)_3]$, 92397-48-3; $(\text{CH}_3)_3\text{C}_6\text{CH}_2\text{C}_6(\text{CH}_3)_4\text{H}$, 92397-51-8; $(\text{CH}_3)_4\text{C}_6\text{HCH}_2\text{C}_6(\text{CH}_3)_3\text{H}_2$, 23946-68-1; LiO_2CCF_3 , 2923-17-3; hexamethylbenzene cation radical, 34473-51-3; prehnitene dimer cation radical, 92397-49-4; pentamethylbenzene dimer cation radical, 92397-50-7; pentamethylbenzene-*d*, 16032-49-8; durene-2,5-*d*, 1859-01-4; mesitylene-2,4,6-*d*, 38574-14-0; pentamethylbenzyl trifluoroacetate, 35843-80-2; pentamethylphenyl trifluoroacetate, 1683-07-4; mesitylene, 108-67-8; durene, 95-93-2; pentamethylbenzene, 700-12-9; hexamethylbenzene, 87-85-4; deuterium, 7782-39-0.

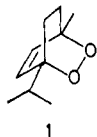
Mechanism of Endoperoxide Formation. 3. Utilization of the Young and Carlsson Kinetic Techniques¹

Edward L. Clennan* and M. E. Mehrsheikh-Mohammadi

Contribution from the Department of Chemistry, The University of Wyoming, Laramie, Wyoming 82071. Received March 7, 1984

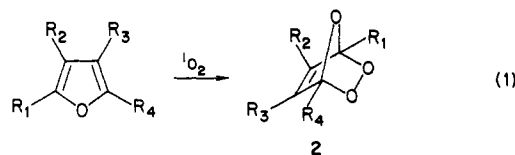
Abstract: The rate constants for the additions of singlet oxygen to 39 furans and cyclopentadienes have been determined. The effect of substituents on the observed rate constants was interpreted to suggest that the geometry of singlet oxygen addition is influenced by electron density distributions. The formation of endoperoxides was also compared to the Diels-Alder reaction. The different character of these reactions is compelling evidence for the presence of exciplexes on the reaction surfaces for the formation of endoperoxides.

In 1908 Gutig² isolated a compound which was identified in 1912 by Wallach³ as ascaridole (**1**). At the time this was the



only structurally established transannular peroxide. The rational synthesis of endoperoxides by 4 + 2 cycloadditions of singlet oxygen and dienes, however, was not accomplished until 1926,

when Dufraisse published his first⁴ of many papers in this area.⁵ In 1952 Schenck reported that the heterocyclic compound furan⁶ and its derivatives (eq 1) also reacted with oxygen in the presence of a sensitizer and light to produce unstable endoperoxides **2**.



(4) Moureu, C.; Dufraisse, C.; Dean, P. M. *C. Hebd. R. Seances Acad. Sci.* **1926**, 182, 1584.

(5) (a) Dufraisse, C.; Rio, G.; Basslier, J.-J. *C. R. Hebd. Seances Acad. Sci.* **1958**, 246, 1640. (b) Dufraisse, C.; Etienne, A.; Basselier, J.-J. *Ibid.* **1957**, 244, 2209. (c) Dufraisse, C.; Etienne, A.; Aubry, J. *Bull. Soc. Chim. Fr.* **1954**, 1201. (d) Dufraisse, C.; Etienne, A.; Aubry, J. *C. R. Hebd. Seances Acad. Sci.* **1954**, 239, 1170.

(6) (a) Schenck, G. O. *Angew. Chem.* **1952**, 64, 12. (b) Schenck, G. O. *Ibid.* **1957**, 69, 579. (c) Schenck, G. O. *Justus Liebigs Ann. Chem.* **1953**, 584, 156. (d) Schenck, G. O. *Chem. Zentr.* **1954**, 6345. (e) Schenck, G. O. *Ibid.* **1955**, 5415.

(1) Preliminary communication of some of these results have appeared: (a) Clennan, E. L.; Mehrsheikh-Mohammadi, M. E. *J. Am. Chem. Soc.* **1983**, 105, 5932. (b) Clennan, E. L.; Mehrsheikh-Mohammadi, M. E. *J. Org. Chem.* **1984**, 49, 1321.

(2) (a) Gutig. *Berichte von Schimmel and Co.* 108 (April 1908); *Chem. Zentralbl.* **1908**, 1, 1839. (b) Arbuzov, Y. A. *Russ. Chem. Rev. (Engl. Transl.)* **1965**, 34, 558.

(3) (a) Wallach, O. *Nachr. Ges. Wiss. Gottingen* **1912**, 422. (b) Wallach, O. *Ann.* **1912**, 392, 54.